An Ultrastructural Study of *Vairimorpha necatrix* (Microspora, Microsporida) with Particular Reference to Episporontal Inclusions During Octosporogony

CLYDE B. MOORE[1] and WAYNE M. BROOKS

Department of Entomology, North Carolina State University, Raleigh, North Carolina 27695-7613

ABSTRACT. The life cycle of *Vairimorpha necatrix* was studied by electron microscopy. Disporous development has two distinct stages: 1) diplokaryotic meronts which are actively mitotic, and 2) diplokaryotic sporonts which are distinguished by reduced ribosome density and a thickened plasmalemma. After final division of the sporont, sporoblasts form spores which are ovocylindrical and measure 4.4 ± 0.08 × 2.3 ± 0.05 μm (mean ± SE). Octosporous development results in eight haploid spores being formed in a sporophorous vesicle. The uninucleate octospores were smaller than the binucleate dispores and the exospore was thicker but less crenulate in outline. Early in octosporogony, tubules are produced from the sporont plasmalemma and electron-dense material accumulates in the episporontal space. The latter may be amorphous, vesiculated, or vacuolated in appearance and in later stages may take a stacked, lamellar form. At sporoblast formation, exospore material coats the plasmalemma and attached tubules; all inclusions in the episporontal space gradually disappear as spores are formed. These secretory products may have application to taxonomic distinction at the species level.

Key words. Life cycle, sporophorous vesicle, tubules.

THE genus *Vairimorpha* was erected in 1976 by Pilley with the dimorphic microsporidium *Vairimorpha necatrix* (Kramer, 1965) as the type species. This microsporidium was first reported by Tanada and Chang [16] as a mixture of two separate species which were subsequently described by Kramer [8] as *Nosema necatrix* and *Thelohania diazoma*. In his intensive study of these isolates, Maddox (Maddox, J. V. 1966. Studies on Microsporidiosis of the Armyworm *Pseudaletia unipuncta* (Haworth). Ph.D. Thesis, Univ. of Illinois, Urbana) indicated the possibility that the two species may only be physiological variants of the same species, a conclusion supported by subsequent studies [2, 11].

In establishing the genus *Vairimorpha*, Pilley [13] redescribed the developmental stages based on Giemsa-stained preparations. The genus was characterized primarily by a dominant developmental cycle involving binary fission and disporoblastic sporogony and an additional cycle involving multiple fission and octosporoblastic sporogony which occurs primarily at low temperatures. Since her work, several additional dimorphic species have been placed in this genus, including *V. plodiae* (Kellen & Lindegren, 1968), *V. heterosporum* (Kellen & Lindegren, 1969), *V. ephestiae* (Mattes, 1927), *V. hybomitrae* (Levchenko & Issi, 1973), *V. invictae* Jouvenaz & Ellis, 1986, *Vairimorpha antheraeae* Yefimenko, 1987, and an isolate referred to as *Vairimorpha* sp. originally discovered by J. J. Hamm from Bolivia [3]. In addition, as noted by Pilley [13], the occurrence of such dimorphic species exhibiting both apansporoblastic and pansporoblastic development undermines the separation of the order Microsporida into the two suborders Apansporoblastina and Pansporoblastina [17].

Larsson [9, 10] addressed the need to use ultrastructural cytology in defining microsporidian taxa and in developing systems for their classification. However, in previous comparative studies of various species of *Vairimorpha*, biochemical and immunological techniques have been used primarily to distinguish between species (see review in [6]). Observations on ultrastructural cytology have been limited to *V. plodiae* [12], *V. ephestiae* [18], and *V. invictae* [7]. The lack of published observations on the ultrastructural features of the type species, *V. necatrix*, seriously limits our ability to make comparative observations among species in the genus *Vairimorpha*. Such data would provide a more definitive generic characterization based on ultra-

structural cytology. It is to these ends that the present study on the ultrastructural cytology of *V. necatrix* was undertaken.

MATERIALS AND METHODS

A sample of *V. necatrix* spores was received from Dr. J. V. Maddox of the Illinois Natural History Survey. The spore suspension (50 μl of 1 × 10^8 spores/ml) was given per os to 4-day-old larvae of *Helicoverpa zea* from a colony maintained at the North Carolina State University insectary. The larvae were maintained on a synthetic diet [1]. Cohorts of the exposed larvae were kept in environmental chambers (14:10 L:D) at both 25° C and 20° C. Samples of primarily adipose tissue were taken from larvae at 1, 3, 7, 10, 18 and 24 days post exposure. Tissues were fixed in 2.5% cacodylate buffered glutaraldehyde (pH 7.4) overnight at 4° C. Samples were rinsed three times in 0.1 M cacodylate buffer (pH 7.4), and then post-fixed in 1% OsO$_4$ in 0.1 M cacodylate buffer for 2 h. They were rinsed three times, 15 min each, in distilled water and dehydrated through a graded ethanol series. Propylene oxide was used as the transition solvent to embedment in Spurr's low viscosity resin (Ladd Research Industries, Inc., Burlington, VT).

Thin sections, 60–90 nm, were cut on a Reichert OM-2 ultramicrotome. The sections were stained using 5% (w/v) uranyl acetate in 50% (v/v) methanol followed by lead citrate [14]. Sections were examined with a Philips 300 transmission electron microscope at 80 kV.

RESULTS

Meronts were relatively undifferentiated cells containing a single diplokaryon and lay directly in the host cell cytoplasm. They were roughly spherical to elliptical and ranged in size from 1.5 to 3.2 μm. The cytoplasm was evenly dense with ribosomes and contained a few cisternae of rough endoplasmic reticulum (RER) (Fig. 1). Host cell mitochondria were often closely associated with the parasite's plasmalemma. Spindle plaques and microtubules were frequently observed, indicating active mitosis in this stage. In some cases rapid mitotic division resulted in chain-like forms where cytokinesis was delayed. These appeared to be late stage meronts or possibly presporonts as indicated by an increase in cisternae of RER and a slightly thickened plasmalemma (Fig. 2).

Early stage sporonts were identified by their less dense cytoplasm. The plasmalemma also became thickened in areas as electron-dense material was secreted to the exterior eventually forming a continuous layer over the entire surface of the sporont (Fig. 3). The nuclei replicated and at least one additional mitotic

---

[1] To whom correspondence should be addressed.
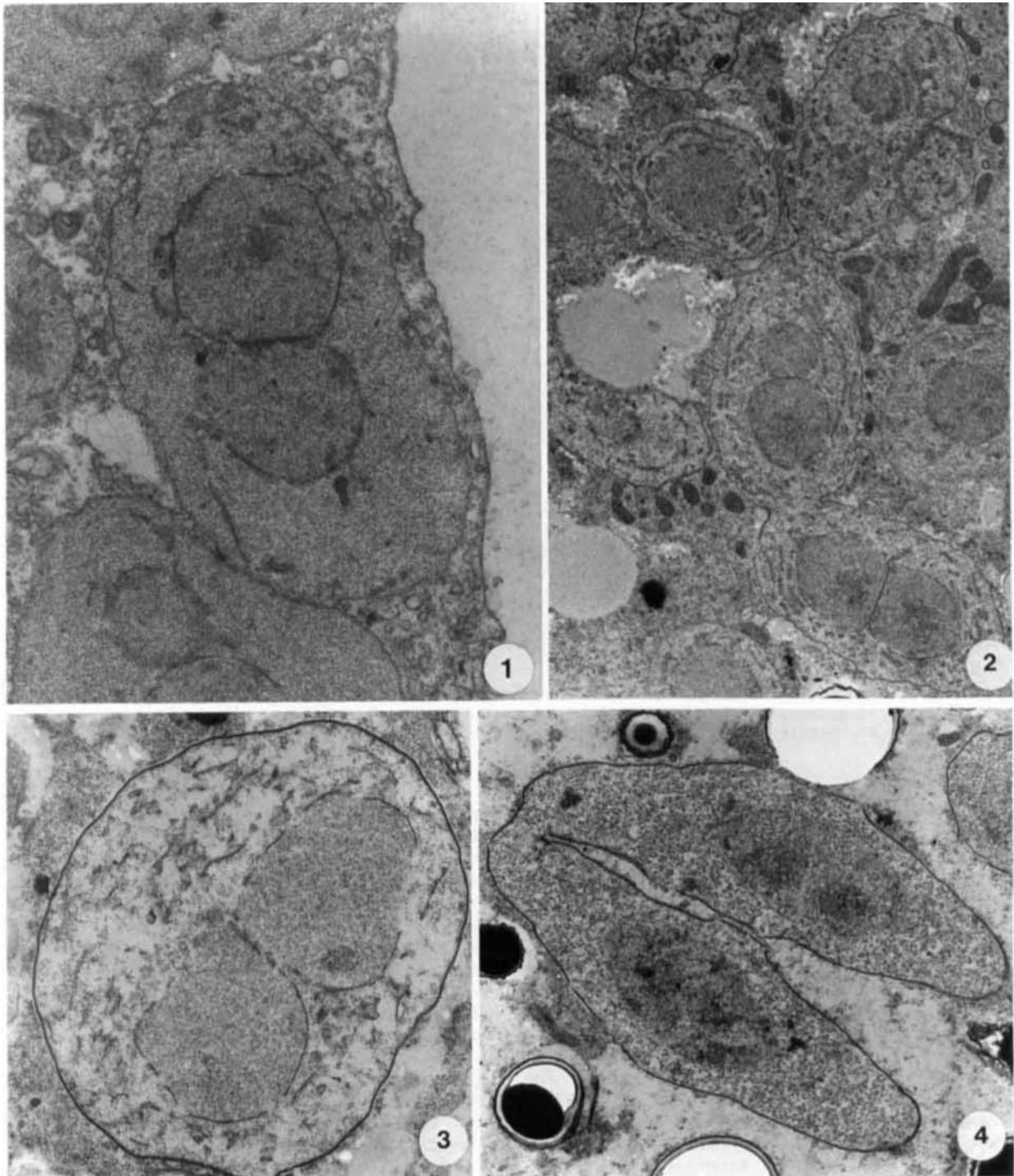
Fig. 1–4. Electron micrographs of *V. necatrix*. 1. Diplokaryotic meront. ×20,500. 2. Chain of three apparently late stage meronts. Note slightly thickened plasmalemma and the abundance of cisternae of rough endoplasmic reticulum. ×11,000. 3. Early diplokaryotic sporont distinguished by thickened plasmalemma and less dense cytoplasm due to decrease in the ribosome density. ×22,500. 4. Dividing sporont. ×12,500.

division appeared to take place (Fig. 4). Cisternae of RER continued to increase and primordial structures of the mature spore began to appear in sporoblasts (Fig. 5). Anteriorly, the anchoring disc of the polar filament formed and the isofilar polar tubule projected posterolaterally, coiling on the average 13 turns (range 12–14) around the centrically located diplokaryon (Fig. 6). The polar filament in cross-section was composed of six concentric

layers, alternately electron lucent and dense, with an inner core (Fig. 6, inset). The diameter of the polar filament was 76 ± 0.2 nm (mean ± SE). The polaroplast appeared as petal-like membranous folds surrounding the basal portion of the polar filament. Posteriorly, a vacuole was usually present and frequently a Golgi apparatus was apparent.

Fresh spores were ovocylindrical, slightly pointed anteriorly
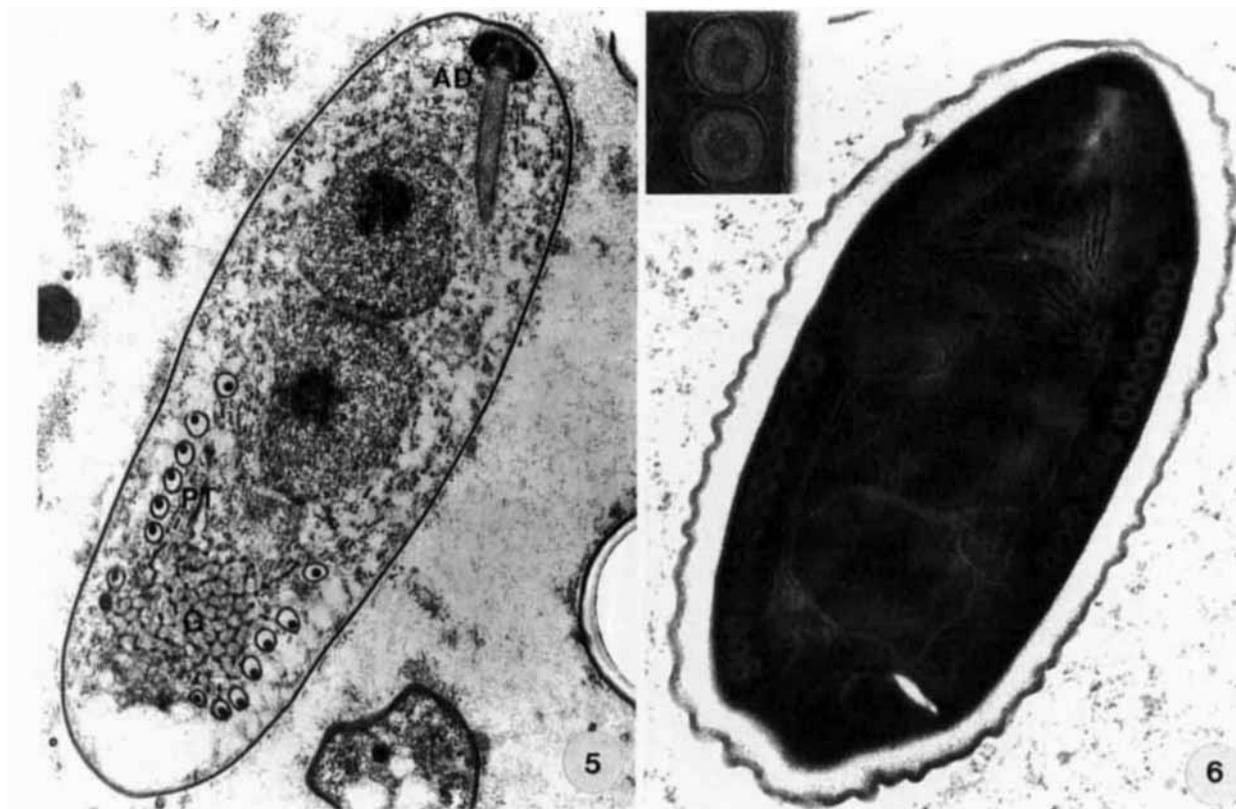
Fig. 5, 6. Ultrastructure of sporoblast and spore of *V. necatrix*. 5. Diplokaryotic sporoblast showing anterior anchoring disc (AD), polar tube primordia (PT), and the Golgi apparatus (G). ×18,000. 6. Mature dispore with polar tube coiling posterolaterally around central diplokaryon. Polaroplast lamellae are evident anteriorly. ×18,000. Inset: enlargement of polar filament in cross section. ×70,000.

and measured 4.4 ± 0.08 × 2.3 ± 0.05 μm. The outermost layer of the spore coat, the exospore, was electron dense, 24 nm thick, and appeared crenulate (Fig. 6). The electron-lucent endospore layer was uniformly 160 nm thick except anteriorly where the anchoring disc was attached.

While stages in octosporogony were occasionally seen in material which had been held at 25° C, these stages were most abundant in material held at 20° C. Early octosporonts were similar in appearance to the diplokaryotic sporonts where the cytoplasm was less dense and cisternae of RER became more abundant (Fig. 7). The principal distinction was the formation of a membrane-like structure exterior to the plasmalemma that became the envelope of the sporophorous vesicle (SV). The envelope appeared as blebs at various places on the plasmalemma and electron-dense material was secreted into the episporontal space (ES) between the envelope and the sporont plasmalemma (Fig. 7). As shown when examined in a favorable plane of section (Fig. 8, 9), these early octosporonts were binucleate. Separation of the two nuclei of the diplokaryon prior to meiosis is apparent in Fig. 8 and 9, but synaptonemal complexes indicating meiotic activity were not observed. Following this stage, nuclear division and cytokinesis gave rise to tetra- and octonucleate sporonts. Spindle plaques with microtubules radiating toward electron-dense chromatin masses, probably synapsed chromosomes, were observed in dividing nuclei (Fig. 10).

The cytoplasm of the early stage sporonts was observed containing material in vacuoles similar to the electron-dense material secreted into the ES (Fig. 9, 11). This secretory material

ranged from being uniformly electron dense to more-or-less vacuolated in appearance (Fig. 8–11). In some sporonts the electron-dense material appeared to organize into lamellar structures (Fig. 12, 13) 21 to 34 nm (27 ± 0.01) thick. In more advanced stages of octosporogony (Fig. 14), the lamellae either disappeared or reorganized into the electron-dense amorphous masses of secretory material. Alternatively, this material may not always organize into lamellae and may persist in the ES during sporoblast formation.

Tubular structures, 23–49 nm (36 ± 0.8) in diameter, also occurred in the ES primarily in the space between the sporont and the secretory material (Fig. 10–12); in some sections, they appeared to have been produced from or attached to the sporont plasmalemma (Fig. 15). The faintly staining tubules were usually closely associated with the secretory material but separate groups of tubules often occurred apart from this material. The tubules also occurred in sporonts exhibiting the stacked lamellae and usually persisted in the ES during sporoblast formation (Fig. 13).

Sporoblast development was marked by an increasingly electron-dense and thickened layer of exospore material on the sporont plasmalemma (Fig. 13–16). As the exospore was deposited on the surface of the plasmalemma, it also coated the basal regions of the tubules still attached to the sporont plasmalemma (Fig. 16). Tubules and secretory material gradually disappeared with sporoblast formation and spore maturation (Fig. 17, 18).

Relatively few of the mature spores formed during octosporogony were well fixed and/or infiltrated with embedment. Many of the octospores appeared to be aberrant and internal detail
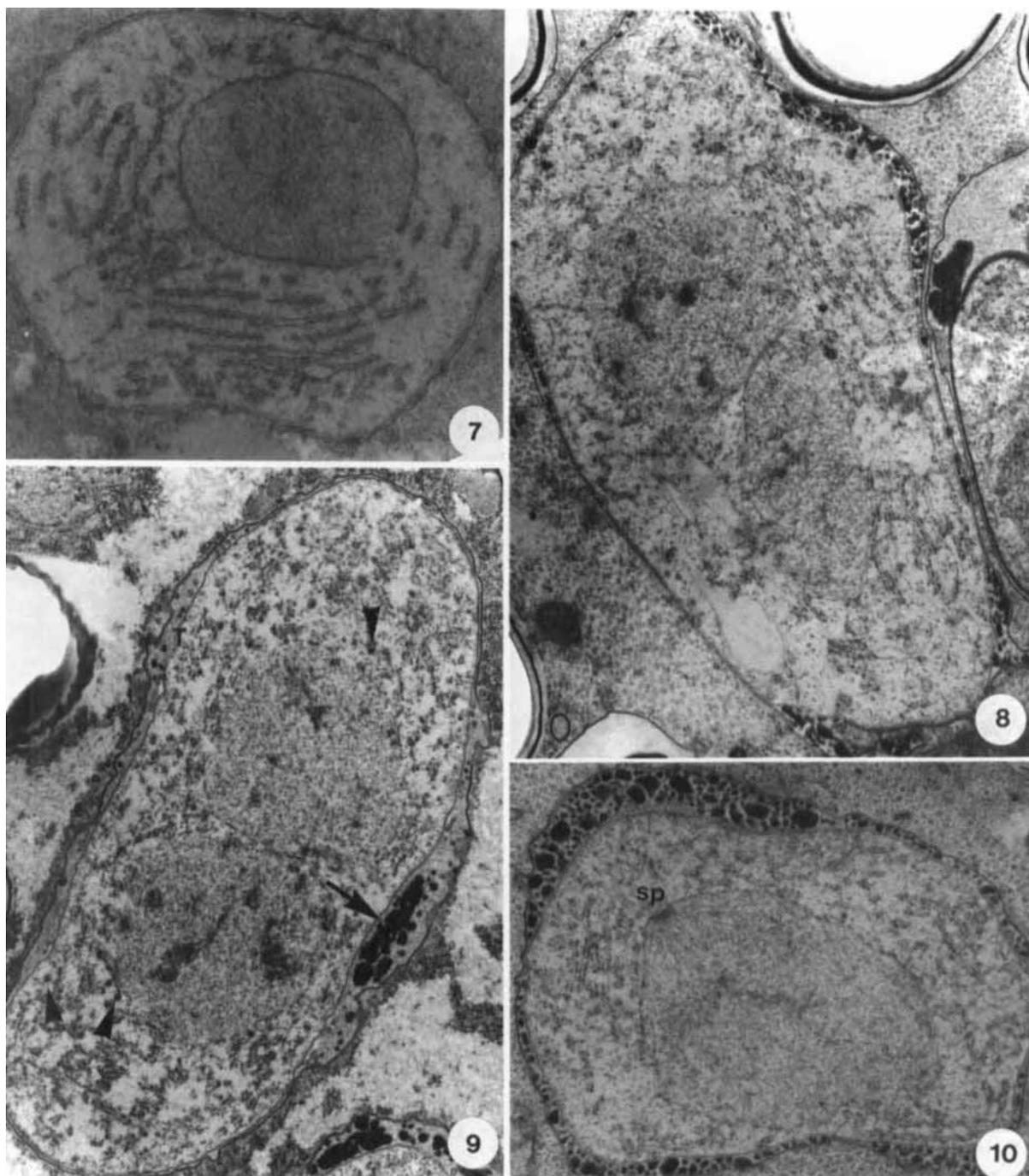
Fig. 7–10. Electron micrographs of early stages in octosporogony of *V. necatrix*. 7. Initial octosporont within a sporophorous vesicle. Note presence of secretory material in the episporontal space between the sporont and the envelope of the sporophorous vesicle. ×15,000. 8. Binucleate sporont. Note area of apposition between the paired nuclei of the diplokaryon. ×16,500. 9. A sporont whose nuclei are beginning to separate prior to meiosis. Note tubules (T) and amorphous masses of secretory material (arrow) in the episporontal space. Vacuoles (arrowheads) also are present in the cytoplasm which contain material similar to the electron-dense secretory masses that occur in the episporontal space. ×16,500. 10. Sporont undergoing division. Note spindle plaque (sp) with microtubules radiating toward chromatin masses. ×19,000.

was best preserved in immature spores. The polar filament was isofilar, exhibited 12 to 13 coils (Fig. 18) and in cross section was similar to that of the diplokaryotic spores, measuring 76 ± 0.9 nm in diameter. An exospore layer overlaid the much thicker endospore. Fresh spores measured 3.8 ± 0.04 × 2.1 ± 0.03 μm.

DISCUSSION

The life cycle of *V. necatrix* does not appear to differ significantly from that described by Pilley [13] or for *V. plodiae* [12]. Meronts are typically undifferentiated as reported for many microsporidia and are mitotically active. A principal feature of
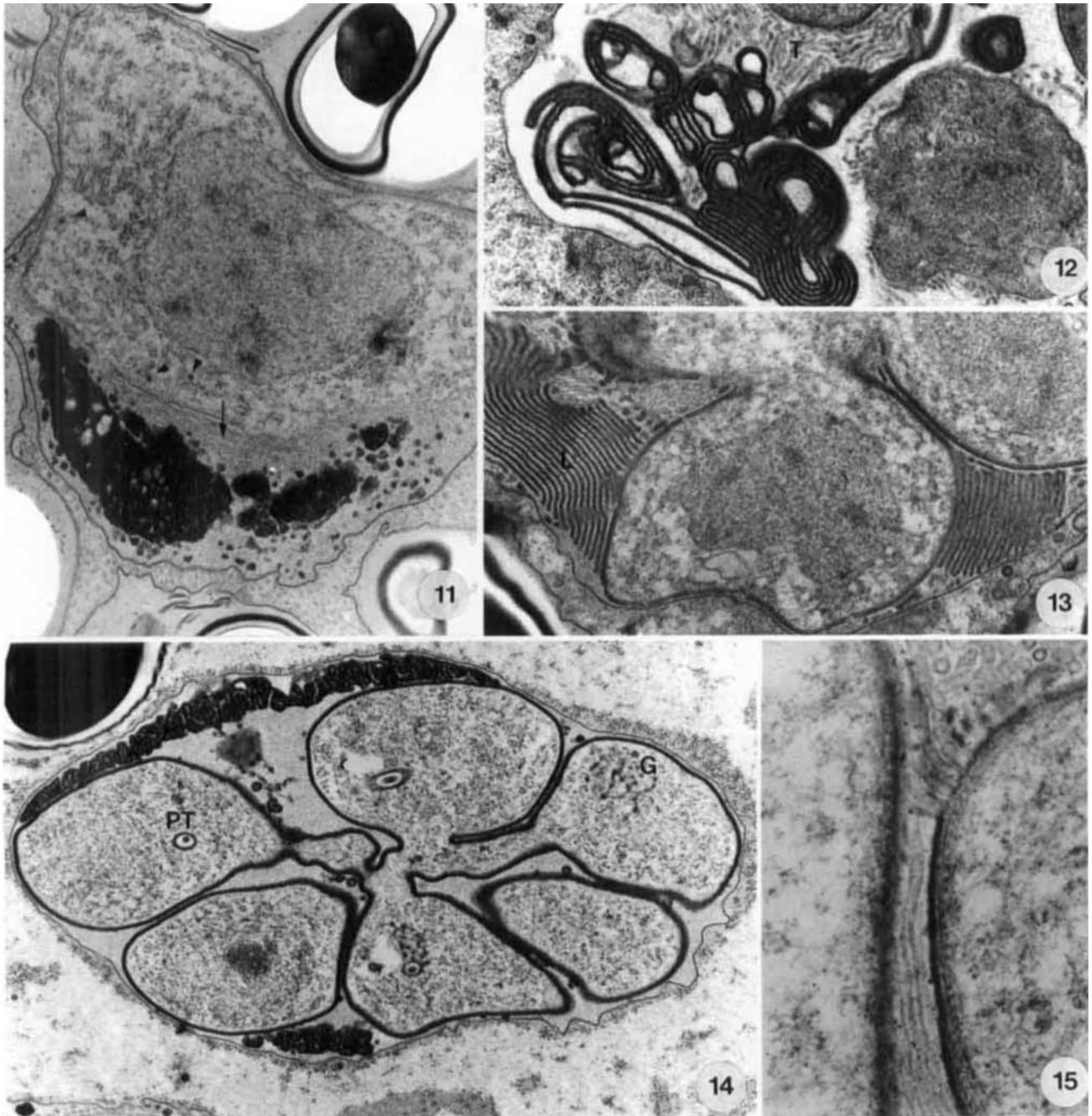
Fig. 11–15. Electron micrographs of sporogonic stages of *V. necatrix*. **11.** Sporont with extensive mass of tubules (arrow) between the sporont plasmalemma and the masses of amorphous secretory material in the episporontal space. Note the secretory material is vesiculate in appearance. Vacuoles (arrowheads) containing apparent secretory material can also be seen in the sporont cytoplasm. ×19,800. **12, 13.** Appearance of stacked lamellae (L) in the episporontal space of sporont along with tubules (T). ×18,700. **14.** Advanced sporont with six sporoblasts evident in the plane of section. Note greatly thickened plasmalemma of the sporoblasts, presence of polar filament primordia (PT) and Golgi apparatus (G), and reduced presence of tubules. ×16,500. **15.** Attachment of tubules to sporont plasmalemma. ×62,000.

meronts and disporogonial stages is the presence of diplokarya. While cells often appear uninucleate in electron micrographs, this is most likely due to the plane of section. Likewise, daughter meronts are more often encountered with one in the plane of section and the second in transverse section. This and micrographs of early cleavage indicate that division is at an obtuse angle, although longitudinal division is seen in some cases. In both situations, mirror-image symmetry is the usual condition.

The spindle plaques, polar vesicles and microtubules of mitosis were not observed in detail or proper plane of section in order to further describe these structures; however, Malone and Canning's [12] work and Larsson's [9] review on ultrastructure indicate that these structures in this species would not likely differ.

Although no direct evidence was obtained, the early stages of octosporogony are believed to be meiotic. Synaptonemal com-
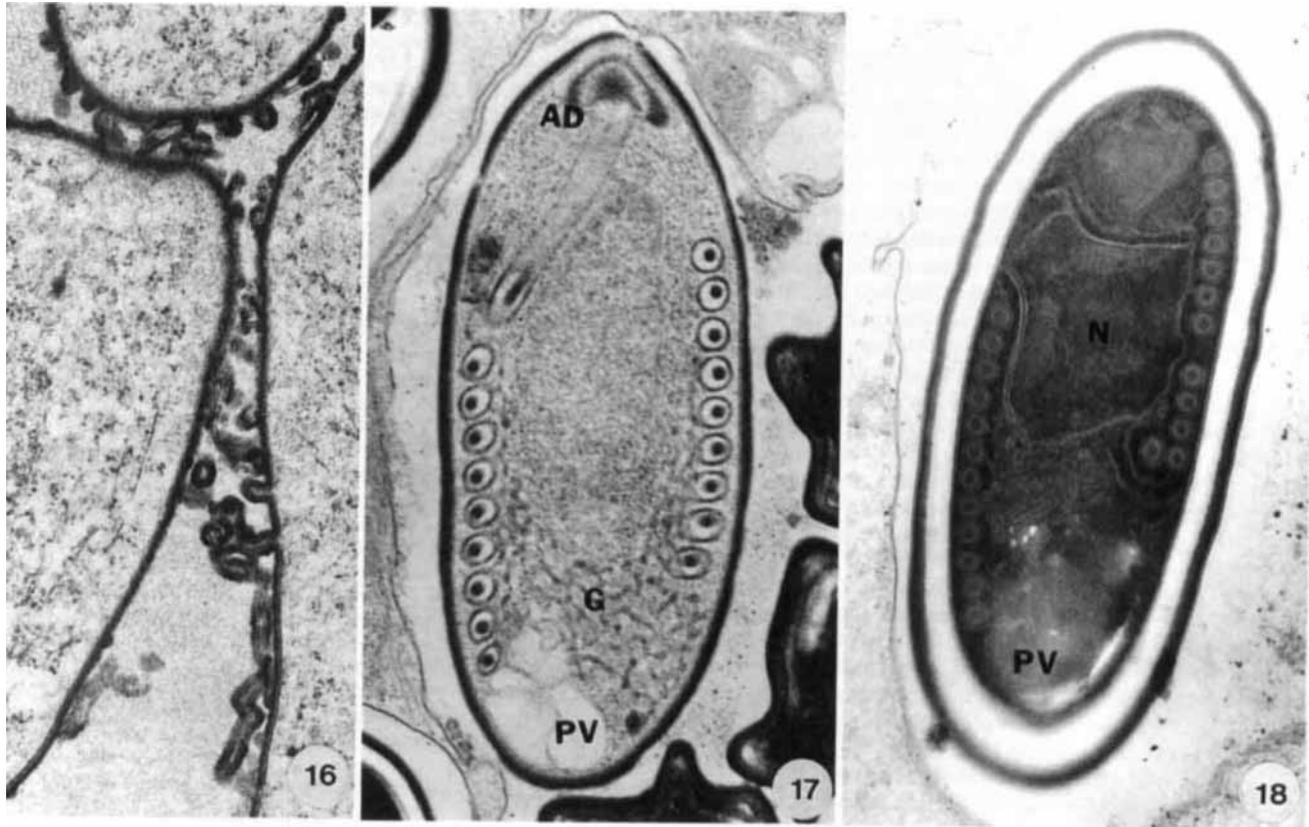
Fig. 16–18. Electron microgrographs of advanced stages in octosporogony of *V. necatrix*. 16. Sporoblasts with tubules attached to the plasmalemma. Note the walls of the tubules have been greatly thickened by the deposition of exospore material on their surface. ×33,500. 17. Sporoblast showing anchoring disc (AD) and coils of the polar filament, Golgi apparatus (G), and posterior vacuole (PV). ×30,000. 18. Mature octospore, nucleus (N), posterior vacuole (PV). ×30,000.

plexes were found in early octosporonts of *V. plodiae* by Malone and Canning [12], and they have also been described in species of the dimorphic genera *Amblyospora* and *Parathelohania* [4, 5]. In *V. necatrix* we did not observe karyogamy, but diplokaryotic sporonts and sporonts whose nuclei were undergoing disassociation prior to meiosis were observed (Fig. 8, 9). Better preservation of structures in such nuclei might have allowed resolution of the synaptonemal complexes.

Various types of inclusions occur within the ES during octosporogony (Fig. 8–18). Working with a *Glugea* sp., Takvorian and Cali [15] identified three types of tubular appendages continuous with the sporont's plasmalemma. Larsson [9] has reviewed other types of inclusions described in the ES of other species. In *V. necatrix*, Type II tubules of Takvorian and Cali's classification were observed. These clearly emanate from the plasmalemma of the sporont (Fig. 15) and are most abundant in early stages of octosporogony (Fig. 9–13). Malone and Canning [12] described these as being parallel to the plasmalemma. In our study, tubules were most frequently seen in close association with the plasmalemma but not necessarily parallel. Frequently the tubules extended further into the ES with little apparent organization. Although these tubules have mostly disappeared in late octosporogonic stages, tubules still attached to the sporont plasmalemma when exospore material is deposited externally on developing sporoblasts are also coated basally (Fig. 16).

The tubules are usually present and may be closely associated with the amorphous secretory material which accumulates early in the ES (Fig. 11–13). The electron-dense material occurs initially in small deposits between the sporont plasmalemma and the newly formed envelope of the sporophorous vesicle in early octosporonts (Fig. 9, 11). As the tubules appear subsequently, it seems unlikely that the tubules play a role in the formation of the amorphous secretory material. Rather, this material is probably formed within the sporont itself. Similar electron-dense material occurring within membrane-bound vacuoles is common in the cytoplasm of the sporonts (Fig. 8, 9, 11) and is probably released by the process of exocytosis.

The amorphous secretory material is usually electron dense and may become vacuolated as well as vesiculate in appearance (Fig. 11). At some point during sporogony, this material may organize into lamellae with a stacked-layered appearance (Fig. 12, 13). However, as deposits of the amorphous material occur frequently in late stage octosporonts (Fig. 14), either the material does not always organize into lamellae or it changes back into its original nature before gradually disappearing along with the tubules during spore formation.

Takvorian and Cali [15] suggested that tubules (appendages) such as these be avoided as taxonomically significant features until more study has been completed. We feel that these may be useful in taxonomy, especially at the species level. For example, they are the one morphological difference which can be used to distinguish between *V. necatrix* and *V. plodiae*, species which are otherwise difficult to separate by ultrastructure. The SV inclusions, which are amorphous, and the tubules appear identical in each of these species, although the tubules of *V. necatrix* do not appear as tightly associated with the plasmalemma as do those of *V. plodiae*. However, the electron-dense

lamellar structures are the most significantly different feature between these two species. In *V. plodiae* they make "intricate layered configuration(s)" which at the peak of development make fingerprint-like whorls in and around themselves. In *V. necatrix*, the lamellae are more parallel with a stacked membranous appearance (Fig. 13). In Larsson's [9] work on ultrastructural cytology, they would require some expansion of the Type 5E in his description of inclusions in sporophorous vesicles.

The potential taxonomic value of inclusions in the ES is also shown when those occurring in *V. necatrix* are compared with those produced by *V. ephestiae* as described by Weiser and Purrini [18]. In their study, the electron-dense secretory material also transforms into membranous layers similar in configuration to those of *V. necatrix*. The Type II tubules of Takvorian and Cali [15] also are present with both inclusions disappearing during late stages of octosporogony. However, in their study each lamella was identified as having a well-organized central core and two identical surface layers, details not ascertained in *V. necatrix*. While Weiser and Purrini [18] made no attempt to differentiate their species from any of the other described species of *Vairimorpha*, the only significant difference other than that noted above was in the number of coils of the polar filament, apparently 16, of the binucleate spore, although they cite 14 coils in the summary of their paper for both types of spores. They also described stages involved in both disporogony and octosporogony as developing within "parasitophorous vacuoles" of host cell origin; however, this observation needs reinterpretation, especially since their figure of a diplokaryotic sporont (Fig. 37 in [18]) in a "parasitophorous vesicle" complete with tubules and masses of electron-dense secretory material is more likely an early stage in octosporogony prior to meiosis similar to the stage shown in Fig. 8 and 9 in *V. necatrix*. Thus, while the two species appear to be similar ultrastructurally, further study will be required to determine if *V. ephestiae* might be conspecific with *V. necatrix*.

LITERATURE CITED

1. Berger, R. S. 1963. Laboratory techniques for rearing *Heliothis* species on artificial medium. *USDA, ARS (Ser.)*,33-84:4 pp.

2. Fowler, J. L. & Reeves, E. L. 1974. Spore dimorphism in a microsporidian isolate. *J. Protozool.*, 21:538–542.

3. Hamm, J. J., Nordlund, D. A. & Mullinix, B. G. 1983. Interaction of the microsporidium *Vairimorpha* sp. with *Microplitis croceipes* (Cresson) and *Cotesia marginiventris* (Cresson) (Hymenoptera: Braconidae), two parasitoids of *Heliothis zea* (Boddie) (Lepidoptera: Noctuidae). *Environ. Entomol.*, 12:1547–1550.

4. Hazard, E. I., Andreadis, T. G., Joslyn, D. J. & Ellis, E. A. 1979. Meiosis and its implications in the life cycle of *Amblyospora* and *Parathelohania* (Microspora). *J. Parasitol.*, 65:117–122.

5. Hazard, E. I. & Brookbank, J. W. 1984. Karyogamy and meiosis in an *Amblyospora* sp. (Microsporida) in the mosquito *Culex salinarius. J. Invertebr. Pathol.*, 44:3–11.

6. Irby, W. S., Huang, Y. S., Kawanishi, C. Y. & Brooks, W. M. 1986. Immunoblot analysis of exospore polypeptides from some entomophilic microsporidia. *J. Protozool.*, 33:14–20.

7. Jouvenaz, D. P. & Ellis, E. A. 1986. *Vairimorpha invictae* n. sp. (Microspora: Microsporida), a parasite of the red imported fire ant, *Solenopsis invictae* Buren (Hymenoptera: Formicidae). *J. Protozool.*, 34:457–461.

8. Kramer, J. P. 1965. *Nosema necatrix* sp. n. and *Thelohania diazoma* sp. n., microsporidians from the armyworm, *Pseudaletia unipuncta* (Haworth). *J. Invertebr. Pathol.*, 7:117–121.

9. Larsson, R. 1986. Ultrastructure, function and classification of microsporidia. *Progr. Protistol.*, 1:325–390.

10. Larsson, R. 1988. Identification of microsporidian genera (Protozoa, Microspora). A guide with comments on the taxonomy. *Arch. Protistenkd.*, 136:1–37.

11. Maddox, J. V. & Sprenkel, R. K. 1978. Some enigmatic microsporidia of the genus *Nosema. Misc. Publ. Entomol. Soc. Am.*, 11: 65–84.

12. Malone, L. A. & Canning, E. U. 1982. Fine structure of *Vairimorpha plodiae* (Microspora, Burenellidae), a pathogen of *Plodia interpunctella* (Lepidoptera, Phycitidae) and infectivity of the dimorphic spore. *Protistologica*, 28:503–516.

13. Pilley, B. M. 1976. A new genus, *Vairimorpha* (Protozoa: Microsporida) for *Nosema necatrix* Kramer 1965: pathogenicity and life cycle in *Spodoptera exempta* (Lepidoptera: Noctuidae). *J. Invertebr. Pathol.*, 28:177–183.

14. Sato, T. 1968. A modified method for lead staining. *J. Electron Micros.*, 16:133.

15. Takvorian, P. M. & Cali, A. 1983. Appendages associated with *Glugea stephani*, a microsporidian found in flounder. *J. Protozool.*, 30: 251–256.

16. Tanada, Y. & Chang, G. Y. 1962. An epizootic resulting from a microsporidian and two virus infections in the armyworm, *Pseudaletia unipuncta* (Haworth). *J. Invertebr. Pathol.*, 4:128–131.

17. Tuzet, O., Maurand, J., Fize, A., Michel, R. & Fenwick, B. 1971. Proposition d'un nouveau cadra systématique pour les genres de Microsporidies. *C. R. Acad. Sci.*, 272:1268–1271.

18. Weiser, J. & Purrini, K. 1985. Light- and electron microscopic studies on the microsporidian, *Vairimorpha ephestiae* (Mattes) (Protozoa, Microsporida) in the meal moth, *Ephestia kühniella. Arch. Protistenk.*, 130:170–189.

ERRATUM

Please note the following corrections to the article entitled "Factors Influencing *Pneumocystis* Infection in the Immunocompromised Rat," by Melanie Cushion and Michael J. Linke in volume 38, number 6, pages 133S–135S. Page 134S, second column, fourth paragraph, line 3, under Results and Discussion should read as follows: "Of the VAb+ rats that were conventionally housed (Group D), all remained reactive to the 45–50 kDa complex at 6- and 8-wk PI. . . ."

Additionally, in Table 1, in Group B (VAb+, barrier-housed), the rats tested at 10 wk PI were all reactive to the rat coronavirus (3/3 RCV) in addition to 3/3 for PVM. Therefore, the fourth column [Number positive/total number of animals tested (viral antibody present)] should have read 3/3 (PVM), 3/3 (RCV) after the 10 wk PI Group B.